

# Effect of Fasting on Blood Pressure Pulse Transient Time of Healthy Subjects

Omer Hamid, Seedahmed S. Mahmoud, Tareq Al-Hadidi, Sultan Almutawa, Majed Alotibi

**Abstract:** During the month of Ramadan Muslims worldwide fast daily from dawn to dusk. They refrain from consuming food, drinking a liquid, and smoking. In this paper, a pilot study of the effect of fasting on blood pressure pulse transient time (PTT) of healthy subjects is presented. Blood pressure wave transient time referenced to ECG R-wave was measured for a group of seven healthy male subjects one time, in Ramadan during fasting and one time after the month of Ramadan. The Systolic blood pressures, heart rates, and the heights of all recruited subjects were recorded. An ECG and photoplethysmography (PPG) computer-based systems were designed and used in this research. ECG and PPG signals are preprocessed by Whittaker's smoother and their peaks are detected by Pan Tompkins peak detection technique. The pulse transient time was measured at the right and left fingers and toes. After analyzing the results, a paired two samples for means at  $P < 0.05$ , showed that the pulse transient time (PTT) differ significantly in fasting except for the right fingers, where the test was not significant. The coefficients (msec/mmHg) of PTT versus systolic pressure is higher in fasting than in non-fasting conditions with  $p < 0.005$ .

**Index Terms:** ECG R-wave, Fasting, Photoplethysmography, Pulse transient time, Systolic Blood Pressure.

### Abbreviations

Term	Name	Abv.	Name
RFIN	Right Finger	RFINFast	Right Finger Fasting
LFIN	Left Finger	LFINFast	Left Finger Fasting
LFO	Left Foot	LFOFast	Left Foot Fasting
RFO	Right Foot	RFOFast	Right Foot Fasting
RFIN-NF	Right Finger No Fasting	SBpFast	Systolic Blood pressure Fasting
LFIN-NF	Left Finger No Fasting	SBp-NF	Systolic Blood pressure - No Fasting
LFO-NF	Left Foot No Fasting	Ht	Height
RFO-NF	Right Foot No Fasting	SBp-PTT	Systolic Blood pressure - Pulse Transient Time

## I. INTRODUCTION

Millions Muslims worldwide during Ramadan fast daily from dawn to dusk, for 29 to 30 consecutive days. In this month, significant changes in eating habits and sleeping patterns occur which may significantly affect daily blood pressure along with other physiological parameters. The time delay between the electrical activity of the heart (ECG) and the blood pressure wave is an important physiological parameter. Photoplethysmography (PPG) is usually used to measure the blood pressure wave signal. Allen, in [1] overviewed PPG and its, historical background, electronic circuits, current technology, and application. The delay between the ECG R-wave and the PPG is known as pulse transient time (PTT) in literature and utilized in new cuff-less blood pressure systems as discussed in [2]. Different blood pressure models based on PTT are presented in [3]; including linear, Log, inverse and some more, however, the linear method is the most popular individualized calibrated model. Wearability feature for such system is addressed by a new design of a single ECG/PPG sensor in [4]. The technique of cuff-less blood pressure measurement is not error free. Motion artifacts, signal noise, missed R-wave, electrode contact failure, and other limitations are presented in sleep medicine research [5]. However, continuous blood pressure measurement; cannot be performed with conventional blood pressure devices. Tang et al. [6] developed ambulatory blood pressure monitoring based on PTT measurements. Cuff-less technology [7] under development wherein the near future it will be available to the public seeking a better lifestyle and patients requiring continuous care and monitoring of blood pressure.

There are a number of models available and used by many researchers [3]. In the coming sections, the origins of some popular models are explored and simplified.

The pumping action of the heart generates pressure waves that modulate the elastic modulus (E) of the arterial vessels; is given by:

$$E = E_0 e^{\alpha P} \tag{1}$$

Where  $E_0$  is Young's modulus for zero arterial pressure,  $\alpha$  is a vessel parameter (Euler number), and  $P$  is the arterial pressure [8]. Vessels mechanical properties vary among the population and with age and pathology. Moens-Kortweg pressure wave velocity (PWV) [9], in an elastic tube, is given as:

$$PWV = \sqrt{\frac{hE}{\rho d}} = \sqrt{\frac{AdP}{\rho dA}} = \frac{1}{\sqrt{LC(P)}} \tag{2}$$

Manuscript published on 30 June 2019.

\* Correspondence Author (s)

Omer Hamid, Medical Technology Department, Sattam Bin Abdulaziz University, Kindum of Saudi Arabia.

Seedahmed S. Mahmoud<sup>2</sup>, <sup>2</sup>Dept. of Biomedical Engineering, Shantou University, China.

Tareq Al-Hadidi<sup>3</sup>, Medical Technology Department, Sattam Bin Abdulaziz University, Kindum of Saudi Arabia.

Sultan Almutawa<sup>4</sup>, Medical Technology Department, Sattam Bin Abdulaziz University, Kindum of Saudi Arabia.

Majed Alotibi, Medical Technology Department, Sattam Bin Abdulaziz University, Kindum of Saudi Arabia.

© The Authors. Published by Blue Eyes Intelligence Engineering and Sciences Publication (BEIESP). This is an open access article under the CC-BY-NC-ND license <http://creativecommons.org/licenses/by-nc-nd/4.0/>

where  $h$  is the thickness,  $d$  is the diameter,  $A$  is the area of the tube,  $\rho$  is the blood density,  $L = \frac{\rho}{A}$ , and  $C$  is the tube compliance; a function of pressure  $P$ .

A current review of cuff-less blood pressure mathematical models was given in [3].

These models estimate blood pressure from Pulse Arrival Time (PAT) or Pulse Transient PAT is defined as  $PAT = PEP + PTT$ , where  $PEP$  is the Pre-Ejection Period. Combining equations (1) and (2), the Bramwell-Hills and Moens-Kortweg's equation is obtained, representing the relationship between  $P$  and  $PWV$  and hence the "Time Delay" for an artery with a length of  $l$  [10]:

$$PWV = \frac{l}{\text{TimeDelay}} = \sqrt{\frac{hE_0e^{\alpha P}}{\rho d}} \quad (3)$$

This equation shows that as pressure  $P$  increases, pulse velocity increases, given no change in biomechanical vessel properties like vessel diameter and wall thickness. Pulse time delay is, of course, inversely related to pressure. In the literature, there are models used by most researchers in the next paragraph we will explore some of these models.

## II. OVERVIEW OF PTT BASED BLOOD PRESSURE MODELS

### A. The log PTT model

Considering equation (3), the pressure wave velocity (PWV) is given by:

$$PWV = \frac{l}{\text{TimeDelay}} = PWV_0 e^{\left(\frac{\alpha P}{2}\right)}, \quad (4)$$

where the  $\text{TimeDelay} = PTT$ ,  $PWV_0 = \sqrt{\frac{h_0 E_0}{\rho d_0}}$

Where,  $h_0$  and  $d_0$  are the arterial wall thickness and diameter at zero pressure respectively.  $PWV_0$  is considered constant for a particular individual. For unity length, the blood pressure ( $Bp = P$ ) expression becomes:

$$-\ln(\text{TimeDelay}) = \ln(PWV_0) + \frac{\alpha P}{2}$$

$$Bp = b + a * \ln(PTT) \quad (5)$$

where  $a = -\frac{2}{\alpha}$  and  $b = -\frac{2}{\alpha} \ln(PWV_0)$ .

### B. The inverse squared PTT model

The pulse wave, as a driving force pushes blood in the arteries, has a kinetic and gravitational potential energy given by:

$$F \cdot ds = \frac{m \cdot v^2}{2} + m \cdot g \cdot ht, \quad (6)$$

where  $F$  is the force exerted on blood,  $ds$  = two sites distance,  $m$  is the mass of blood,  $v$  is the pulse wave velocity,  $g = 9.81 \text{m/s}^2$  and  $ht$  is the height difference between two sites. The force can also be written in terms of pressure difference:  $F = \Delta Bp \cdot A$

where  $A$  is the cross section area of the artery and

$$\Delta Bp = \frac{m \cdot v^2}{2A \cdot ds} + \frac{m \cdot g \cdot ht}{A \cdot ds} \quad (7)$$

$m/A \cdot ds = \rho$  is the density of blood and  $v$  can be expressed as  $ds/PTT$ . Hence:

$$\Delta Bp = \rho \frac{ds^2}{2PTT^2} + \rho \cdot g \cdot ht \quad (8)$$

The distance  $ds$  can be approximated from patient's height.  $PTT$  is the pulse transit time in seconds. The average blood density  $\rho$  is  $1035 \text{kg/m}^3$ . The pressure drop in the arterial side of circulation accounts for roughly 70% of the total pressure drop in the body [11], hence  $Bp$  is approximately given by:  $Bp = Bp/0.7$

$$Bp = \frac{\rho \frac{ds^2}{2PTT^2} + \rho \cdot g \cdot ht}{0.7} \quad (9)$$

$$Bp = \frac{Ap}{PTT^2} + B \quad (10)$$

In summary, the  $Bp$  can be written in terms of  $PTT$ , with two variables namely  $Ap$  and  $B$ . The variable  $Ap$  can be estimated from the subject's height:

$$Ap = (0.6 \times \text{height})^2 \times \frac{\rho}{1.4} \quad (10.1)$$

$$B = \frac{\rho \cdot g \cdot ht}{0.7} \quad (10.2)$$

The models in equations (5), and (10), have no clinical meaning, as  $PTT$  approaches  $\infty$  or  $0$ . To overcome this problem, a simplified empirical function is developed in [12]:

$$y = c + \frac{b}{\sqrt{(x - a)}} \quad (11)$$

From equation (3), if  $l=1$  then:

$$\text{TimeDelay} = PTT = \frac{1}{\sqrt{\frac{hE_0e^{\alpha Bp}}{\rho d}}} \quad (12)$$

$$PTT = c + \frac{b1}{\sqrt{(Bp - a1)}} \quad (13)$$

$$Bp = a1 + \left(\frac{b1}{PTT - c}\right)^2, \quad (14)$$

where  $a1$ ,  $b1$  and  $c$ ; are subject specific parameters to be found by calibration.

### C. The PTT inverse model

In [13], the static compliance of thoracic and abdominal aorta was measured and a compliance formula was defined as:

$$C(P) = \frac{Cm}{1 + \frac{(P - P_0)^2}{P_1}} \quad (15)$$



where  $C_m = \frac{A_m}{\pi P_1}$ ,  $A_m$  is the maximum cross-sectional area of the aorta at high pressures,  $P_o$ , is the transmural pressure at the inflection point in the pressure-area curve [13]. At this pressure level the compliance curve reaches its maximum,  $C_m$ . Therefore,  $P_o$  is further called 'max-C-pressure'.  $P_1$  is the compliance half-width pressure, i.e. at  $P_1$ , aortic compliance is equal to  $C_m/2$ .

$$C(p) = \frac{A_m}{\pi P_1 \left(1 + \frac{(P - P_o)^2}{P_1}\right)} \quad (16)$$

$$C(P) = \frac{A_m}{\pi(P_1 + (P - P_o)^2)}$$

For higher pressures,  $(P - P_o) > P_1$ :

$$C(P) = \frac{A_m}{\pi(P - P_o)^2} \quad (17)$$

Using equations (2) and (17)

$$PWV = \frac{1}{\sqrt{L} * \sqrt{\frac{A_m}{\pi(P - P_o)^2}}} \quad (18)$$

$$PWV = \frac{P - P_o}{\sqrt{L} \frac{A_m}{\pi}} \quad (19)$$

$$\frac{1}{PTT} = \frac{1}{k12} - \frac{P_o}{k12}$$

where  $k12 = \sqrt{L \frac{A_m}{\pi}}$

$$P = B_p = \frac{k12}{PTT} + P_o \quad (20)$$

#### D. The proportional (linear) PTT model

If the variations in arterial diameter and arterial wall thickness can be ignored, then the blood pressure would relate linearly to the pressure wave time delay along the vessel.

From equation (3), if  $l=1$ :

$$\text{TimeDelay} = \sqrt{\frac{\rho d e^{-\alpha P}}{h E_o}} \quad (21)$$

In [14], it was shown that  $\alpha = 0.008$ .

Assume  $\alpha P < 1$ , by expansion and approximation:

$$\sqrt{e^{-\alpha P}} = 1 - \alpha P/2$$

$$\text{TimeDelay} = (1 - \alpha P/2)/PWV_o = PTT$$

$$P = B_p = \frac{2}{\alpha} - 2PWV_o \cdot \frac{PTT}{\alpha} = B_1 - A_1 \cdot PTT \quad (22)$$

where  $A_1 = 2PWV_o/\alpha$ , and  $B_1 = 2/\alpha$ .

Equation (22) shows that as the blood pressure increases the pressure wave pulse transient time decreases.

#### E. Diastolic blood pressure (DBP) and PTT model

A model relating DBP to PTT was given in [14]. Quoting their derivation here with T as PTT:

From (21)

$$T^2 = \frac{\rho d e^{-\alpha P}}{h E_o}$$

$$T^2 = \frac{e^{-\alpha P}}{PWV_o^2} \quad (23)$$

$$2 \ln T = -2 \ln PWV_o - \alpha P$$

$$P = -\left(\frac{2}{\alpha}\right) * \ln PWV_o - \left(\frac{2}{\alpha}\right) \ln T \quad (24)$$

In a short time the first term is constant

$$dP/dT = (-2/\alpha T) \quad (25)$$

$$\Delta P = (-2/\alpha T) \Delta T \quad (26)$$

$$SBP = SBP_o + \Delta P \quad (27)$$

where  $SBP_o$  is the initial systolic pressure and,

$$SBP = SBP_o - \left(\frac{2}{\alpha T}\right) \Delta T \quad (28)$$

$$SBP = SBP_o - \left(\frac{2}{\alpha T}\right) (T - T_o) \quad (29)$$

Bramwell-Hill equation [15] can be expressed as follows,

$$T = \frac{1}{PWV} = \sqrt{\frac{\rho \Delta V}{V \Delta P}} \quad (30)$$

$$PP = \Delta P = \frac{\rho \Delta V}{VT^2} \quad (31)$$

where  $PP$  is the pressure pulse,  $\Delta V$  = stroke volume, and  $V$  is the blood volume per unit time.

For initial calibration:

$$PP_o = SBP_o - DBP_o = \frac{\rho \Delta V}{VT_o^2} \quad (32)$$

Combining equations (31) and (32):

$$PP = PP_o \cdot \left(\frac{T_o}{T}\right)^2 \quad (33)$$

where the initial blood pressure pulse:

$$PP_o = (SBP_o - DBP_o).$$

We noticed a similarity between equations (8) and (33), with equation (8) shifted in axis by  $\rho \cdot g \cdot ht$  factor.

Furthermore,  $DBP$  can be calculated from Eqs. (29) and (33), after the initial calibration, as follows:

$$DBP = SBP_o - \left(\frac{2\alpha}{T_o}\right) (T - T_o) - (SBP_o - DBP_o) \cdot \left(\frac{T_o}{T}\right)^2 \quad (34)$$

where  $\alpha = 0.008$ , as mentioned earlier [14]. The initial values of the systolic pressure  $SBP_o$ , transient time  $T_o$ , diastolic pressure  $DBP_o$ , are measured at each experiment in this model.



**F. Heart rate and PTT model**

A review of most mathematical models was given in [3], heart rate (HR) correlates with blood pressure as  $Bp = A_o * PTT + B_o * HR + C_o$ , where  $A_o$ ,  $B_o$ , and  $C_o$  are constants. The rest of the models in [3] are more or less variant versions of the above discussed models. We include height in our PTT curve fitting in this research. Blood pressure during fasting was investigated by many researchers in the past with different results and conclusions on whether fasting increases or decreases blood pressure [16-19]. To our knowledge, the effect of fasting, during Ramadan, on PTT was not widely investigated in the literature. PTT is gaining importance as it can estimate arterial stiffness besides blood pressure [20].

**III. THE DEVELOPED ECG AND PPG SYSTEMS DESCRIPTION**

In this paper the ECG and PPG system were developed in-house. The complete block diagrams for the ECG and PPG systems are shown in Fig. 1.0a and 1.0b. The ECG system consists of an instrumentation amplifier (IA gain =10), band pass filter (0.05-100 Hz), high gain amplifier with a gain = 100, DC level shifter to match the signal level to the interface card with input range between 0-2.5V. Fig. 1.0b shows a block diagram of the PPG system. A red LED is used as a light source. A light dependent resistor is used as a photodetector, followed by: a band pass filter of frequency band between 0.05-25Hz, amplifier (gain =100), a DC level shifter and a computer interface card (PICO log – 16 channels, 12 bits).

The signals are digitized at a sampling rate of 1 kHz. The length of the recording is 15 seconds. A DC removal, 60 Hz notch filter and a smoothing (Whittaker's smoother) [21] algorithm were executed as a preprocessing step. A Pan Tompkins open source Matlab script [22] was used for further processing. The PTTs were estimated by detecting, locating ECG/PPG peaks and their time delays. The developed system also measures the heart rate (BPM).

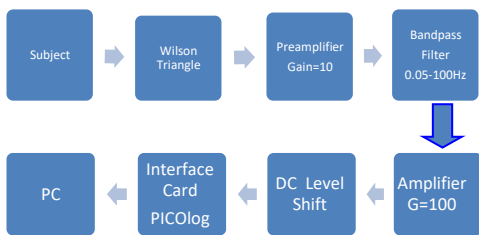


Figure 1.0a ECG System.

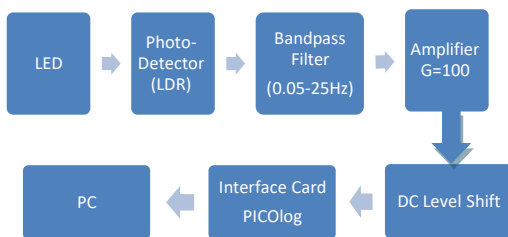


Figure 1.0b PPG System.

**IV. METHOD AND RECORDING PROTOCOL**

A group of 10 male volunteers (age 27±12 years, mean ± sd), participated as a control group in the first part of system

verification and evaluation. Their blood pressures were measured by Medical ECONET Compact 3 device. Subjects' heights (Ht) were also measured. In sitting position, four left/right PPG signals from fingers and toes were measured simultaneously with a number of ECG leads signals, using the above described system. The measurements were performed while the subject was seated on a comfortable chair. The system also measures the heart rates from ECG R-R intervals averaged over 15 seconds. The second part of the measurement involved a group of seven healthy male volunteers (age 39±18 years, mean ± sd). Their PTTs, BPM, Ht, and blood pressures were taken once, approximately in the middle of last month of Ramadan (May-June 2018), and again around two months after Ramadan.

**V. RESULTS AND DISCUSSION**

Fig. 2.0 shows a typical part of ECG and PPG signals. The red lines show the positions of the peaks and the program calculates the time difference (PTT) between consecutive ECG-PPG peaks. Also, the program obtains an averaged heart rate from 15 seconds of ECG signal recording.

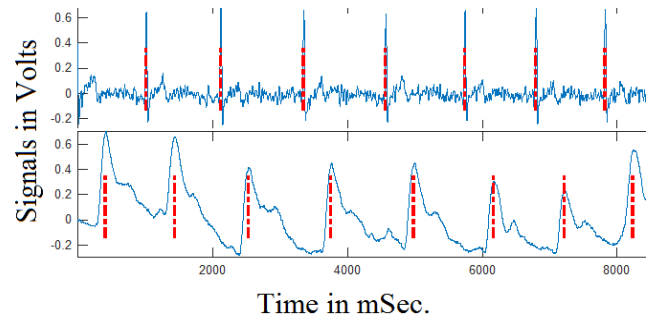


Figure 2.0 ECG QRS and PPG peak detections.

The linear model, equation (22), when compared to the log and the inverse models, the linear model was found to behave well in terms of arterial wall thickness and diameter variations. At the extremities of arterial wall thickness and diameter, the inverse and the log Bp models become unacceptably high or low compared to the linear model, see Fig. 3.0. The following thoracic aorta parameters, at zero pressure [13], were used in obtaining Fig. 3.0: Thoracic aorta wall thickness;  $h_0 = 1.2$  mm, diameter;  $d_0 = 2.85$ cm, Young modulus;  $E_0 = 70000$  Nm<sup>-2</sup>, blood density;  $\rho = 1035$ kgm<sup>-3</sup>, and PTT = 0.3 sec.

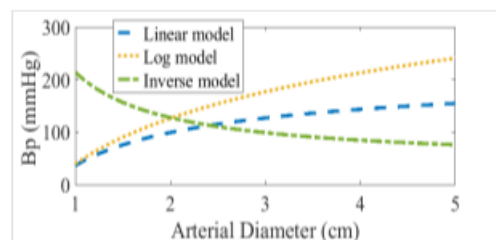


Figure 3.1 Theoretical blood pressure variations as a function of arterial wall diameter, predicted by three models.



The statistics of PTT measurements, mean and standard deviations (std), are given in Table 1.0 for the ten cohorts, which is similar to previous results in the literature [1]. The foot PTT is longer in time as pressure wave traverses the torso.

Fig. 4.0 shows a linear 2-D model fit of PTT as a function of SBp and BPM or Ht. We used the MATLAB curve fitting tool with linear regression to obtain the fit equations associated with Fig. 4.0.

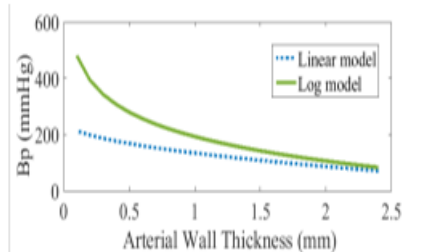


Figure 3.2 Theoretical blood pressure variations as a function of arterial wall thickness, predicted by two models.

Table 1.0 PTTs (Mean ± sd) of the ten cohorts.

LFIN PTT msec	RFIN PTT msec	LFO PTT msec	RFO PTT msec	SBp mmHg	BPM	Ht meters
324 ±22	344 ±25	420 ±20	433 ±21	116 ±7	74 ±14	1.7 ±0.06

The model equations used in the fittings are given below:

$$PTT = C_{SBp} * SBp + C_{BPM} * BPM + C1 \quad (35)$$

$$PTT = C_{SBp} * SBp + C_{Ht} * Ht + C2 \quad (36)$$

$$PTT = C_{BPM} * BPM + C_{Ht} * Ht + C3 \quad (37)$$

We obtained twenty-four coefficients from the model fittings; Table 2.0 lists all the model coefficients and fitting correlation coefficients (R). The PTT slopes  $C_{SBp}$  (msec/mmHg) shown in Table 2.0 are in the same range of slopes' values found in the literature [23].

Table 2.0 2-D model coefficients for the ten cohorts.

Limb PTT as a function of SBp & BPM	$C_{SBp}$ msec/mmHg	$C_{BPM}$ msec/BPM	C1 msec	R
RFO	-1.84	0.03505	644.3	0.6
LFO	-1.815	0.3594	604.5	0.7
RFIN	-0.9177	-0.08766	457.5	0.3
LFIN	-0.1534	-0.3803	370	0.3
Limb PTT as a function of SBp & Ht	$C_{SBp}$ msec/mmHg	$C_{Ht}$ msec/m	C2 msec	R
RFO	-1.378	153.6	326.7	0.7
LFO	-1.511	72.95	469.3	0.7
RFIN	-1.077	-46.58	550.3	0.3
LFIN	-0.7233	-161.3	687.9	0.4

Table 3.0 lists the means and standard deviations of PTTs for fasting and non-fasting seven cohort's measurements. Paired two samples for means at  $p < 0.05$ , showed that the

pulse transient time (PTT) differ significantly in fasting except for the right fingers, where the test was not significant. The measured systolic blood pressure was significantly higher in fasting ( $p < 0.05$ ).

Table 4.0 and Table 5.0 provide the fitting coefficients of equation (35) and (36) models for non-fasting and fasting measurements respectively. The coefficients/slopes (msec/mmHg) of PTT versus systolic pressure is higher in fasting; than in non-fasting conditions with  $p < 0.005$ , it indicates higher PTT sensitivity in fasting. Fig. 5.0 and 6.0 shows the corresponding 2-D surfaces. The results given in Table 2.0 and Table 4.0 are comparable as they belong to non-fasting subjects. PTT as a function of heart rates and the heights (see equation (37)) is plotted in Fig. 7.0 for the seven cohorts. Table 6.0 lists the model coefficients. Table 6.0 shows heart rate has little influence on PPT, but the height influence is dominant as can be seen in Fig. 7.0. Table 7.0 summarizes the t-test results.

Table 3.0 PTT (mean ± sd) for fasting and non-fasting measurements.

PTT locations and subject parameters	mean ±sd non-fasting	mean ±sd fasting
RFO PTT msec	419±31	427±29
LFO PTT msec	414±27	397±37
RFIN PTT msec	352±25	351±12
LFIN PTT msec	342±18	330±17
SBp mmHg	116±9	122±6
BPM	79±11	74±7
Ht meters	1.71±0.06	1.71±0.06

Table 4.0 Non-Fasting model coefficients.

Limb PTT as a function of SBp & BPM	$C_{SBp}$ msec/MmHg	$C_{BPM}$ msec/BPM	C1 msec	R
RFONF	-1.829	-0.005	632.7	0.5
LFONF	-1.993	-0.2863	668	0.7
RFINNF	-0.14	-0.8572	435.5	0.4
LFINNF	0.0103	0.05478	336.3	0.04
Limb PTT As a function of SBp & Ht	$C_{SBp}$ msec/MmHg	$C_{Ht}$ msec/m	C2 msec	R
RFONF	-0.1966	449.7	-324.7	0.9
LFONF	-1.682	116.3	411.1	0.7
RFINNF	-0.14	291.4	-128.8	0.7
LFINNF	-0.0698	-27.99	397.7	0.08

Table 5.0 Fasting model coefficients.

Limb PTT as a function of SBp & BPM	$C_{SBp}$ msec/mmHg	$C_{BPM}$ msec/BPM	C1 msec	R
RFOFAST	-3.788	-0.1	901.9	0.4
LFOFAST	-9.598	-0.1	1600	0.9
RFINFAST	-2.679	-0.5397	713.9	0.4
LFINFAST	-4.255	-0.9055	920.1	0.6
Limb PTT as a function of SBp & Ht	$C_{SBp}$ msec/mmHg	$C_{Ht}$ msec/m	C2 msec	R



# Effect of Fasting on Blood Pressure Pulse Transient Time of Healthy Subjects

RFOFAST	-2.07	413.6	-26.97	0.7
LFOFAST	-8.481	270.5	990.8	0.9
RFINFAST	-2.079	169.6	309.1	0.5
LFINFAST	-3.258	281.9	246.9	0.8

Table 6.0 Equation (37) BPM and Ht coefficients of fasting and non-fasting subjects.

Limb PTT as a function of BPM & Ht	C <sub>BPM</sub> msec/BPM	C <sub>Ht</sub> msec/m	C3 msec	R
RFONF	0	465.3	-374.2	0.9
RFINNF	-0.5058	276.4	-79.84	7
LFONF	-0.4305	227.2	59.88	0.6
LFINNF	0.02798	-21.02	375.5	0.1
RFOFAST	-0.1	455.4	-351.3	0.7
RFINFAST	0.005973	216.6	-32.83	0.5
LFOFAST	-0.1	456.5	-385.5	0.6
LFINFAST	0.001517	355.2	-288	0.6

Table 7.0 Fasting and non-fasting difference t-test summary.

PTT difference	Significance
RFONF – RFOFast	P< 0.05
LFONF - LFOFast	P< 0.05
RFINNF – RFINFast	Not significant
LFINNF – LFINFast	P< 0.05
BpFast – BpNF	P<0.05
(msec/mmHg) Fasting - (msec/mmHg) Non-Fastng	P<0.005

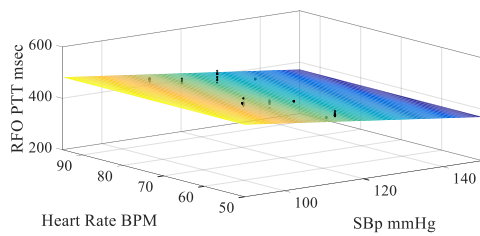


Figure 4.1 Right Foot PTT of 10 subjects. R = 0.6.

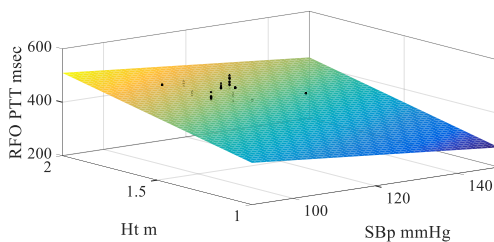


Figure 4.2 Right Foot PTT of 10 subjects. R = 0.7.

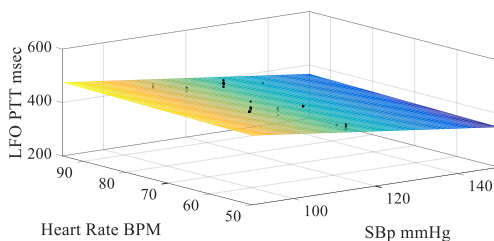


Figure 4.3 Left Foot PTT of 10 subjects. R = 0.7.

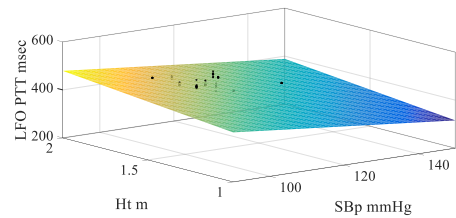


Figure 4.4 Left Foot PTT of 10 subjects. R = 0.7.

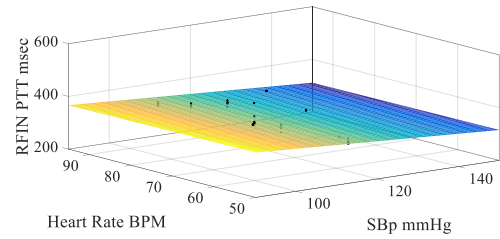


Figure 4.5 Right Finger PTT of 10 subjects. R = 0.3.

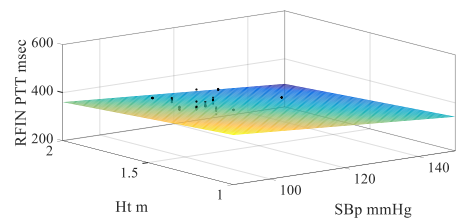


Figure 4.6 Right Finger PTT of 10 subjects. R = 0.3.

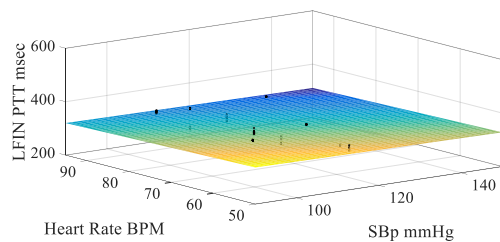


Figure 4.7 Left Finger PTT of 10 subjects. R = 0.4.

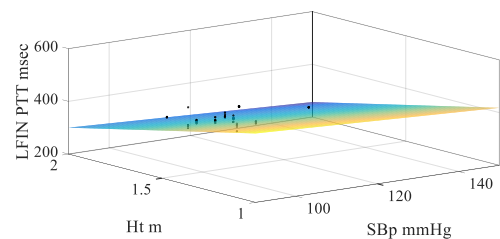


Figure 4.8 Left Finger PTT of 10 subjects. R = 0.4.

Figure 4.0 Ten male subjects (non-fasting) PTT as a function of SBp, BPM and Ht.

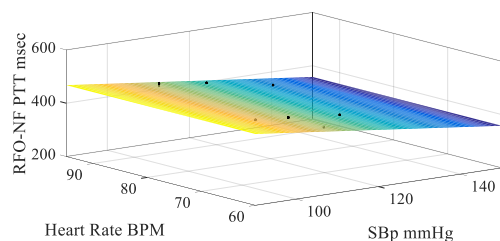


Figure 5.1 Right Foot PTT of 7 non-fasting subjects. R = 0.5.

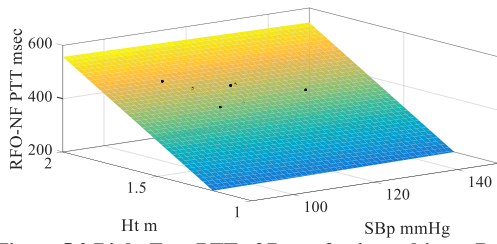


Figure 5.2 Right Foot PTT of 7 non-fasting subjects.  $R = 0.9$ .

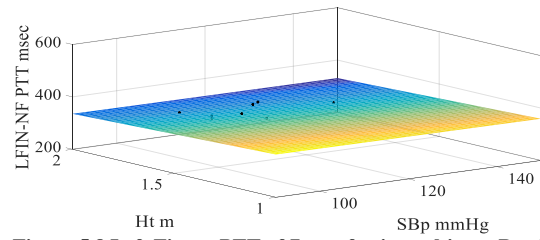


Figure 5.8 Left Finger PTT of 7 non-fasting subjects.  $R = 0.08$ .

Figure 5.0 PTT for 7 subjects when not fasting, as a function of SBp, BPM and Ht.

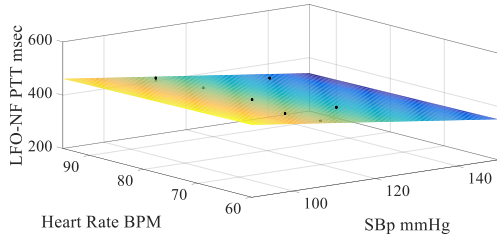


Figure 5.3 Left Foot PTT of 7 non-fasting subjects.  $R = 0.7$ .

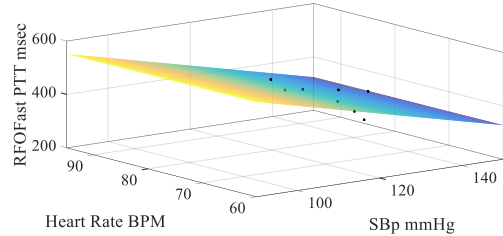


Figure 6.1 Right Foot PTT of 7 fasting subjects.  $R = 0.4$ .

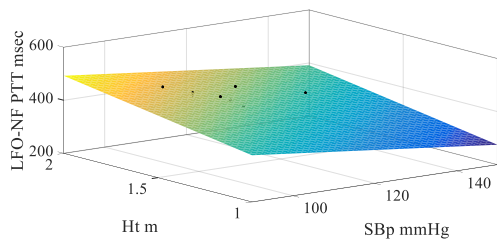


Figure 5.4 Left Foot PTT of 7 non-fasting subjects.  $R = 0.7$ .

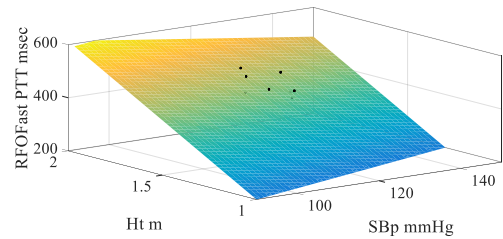


Figure 6.2 Right Foot PTT of 7 fasting subjects.  $R = 0.7$ .

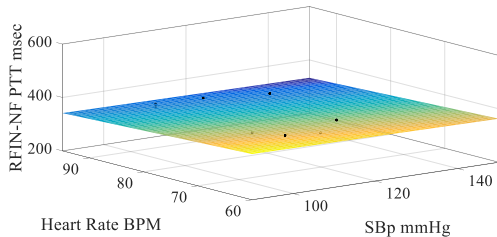


Figure 5.5 Right Finger PTT of 7 non-fasting subjects.  $R = 0.4$ .

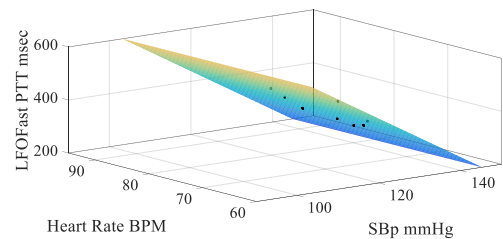


Figure 6.3 Left Foot PTT of 7 fasting subjects.  $R = 0.9$ .

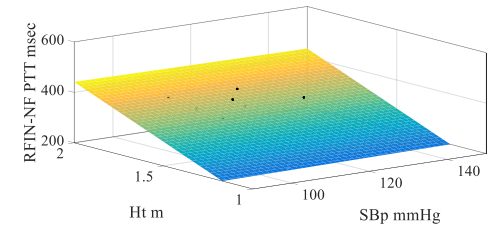


Figure 5.6 Right Finger PTT of 7 non-fasting subjects.  $R = 0.7$ .

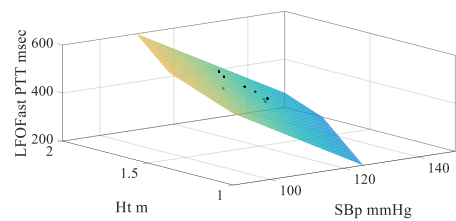


Figure 6.4 Left Foot PTT of 7 fasting subjects.  $R = 0.9$ .

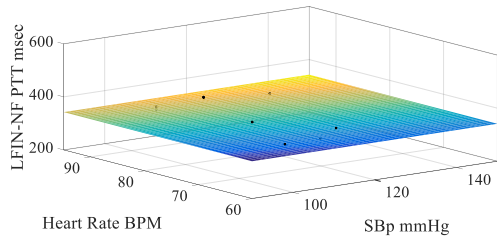


Figure 5.7 Left Finger PTT of 7 non-fasting subjects.  $R = 0.04$ .

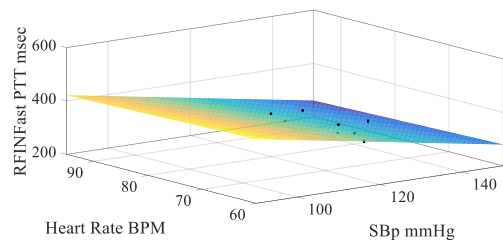


Figure 6.5 Right Finger PTT of 7 fasting subjects.  $R = 0.4$ .

# Effect of Fasting on Blood Pressure Pulse Transient Time of Healthy Subjects

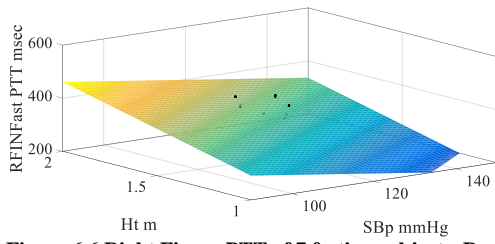


Figure 6.6 Right Finger PTT of 7 fasting subjects.  $R = 0.5$ .

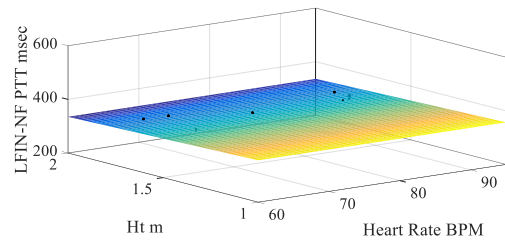


Figure 7.4 Left Finger PTT of 7 non-fasting subjects  $R = 0.1$ .

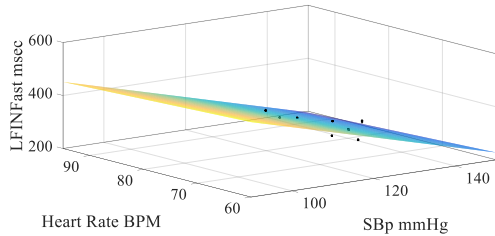


Figure 6.7 Left Finger PTT of 7 fasting subjects.  $R = 0.6$ .

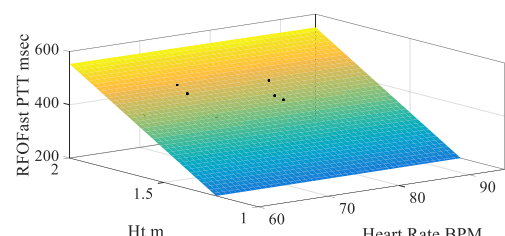


Figure 7.5 Right Foot PTT of 7 fasting subjects  $R = 0.7$ .

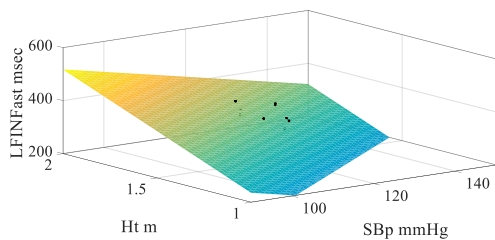


Figure 6.8 Left Finger PTT of 7 fasting subjects.  $R = 0.8$ .

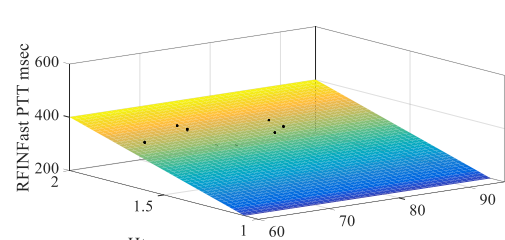


Figure 7.6 Right Finger PTT of 7 fasting subjects  $R = 0.5$ .

Figure 6.0 PTT for 7 subjects when fasting, as a function of SBp, BPM and Ht.

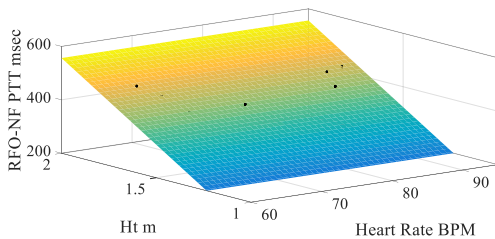


Figure 7.1 Right Foot PTT of 7 non-fasting subjects  $R = 0.9$ .

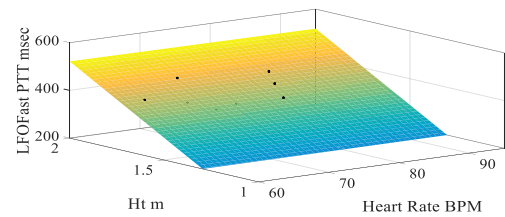


Figure 7.7 Left Foot PTT of 7 fasting subjects  $R = 0.6$ .

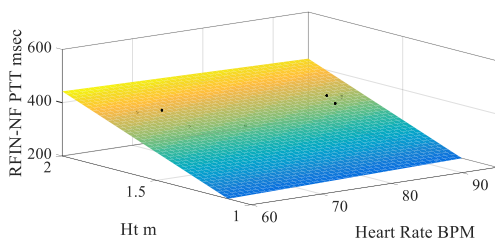


Figure 7.2 Right Finger PTT of 7 non-fasting subjects  $R = 0.7$ .

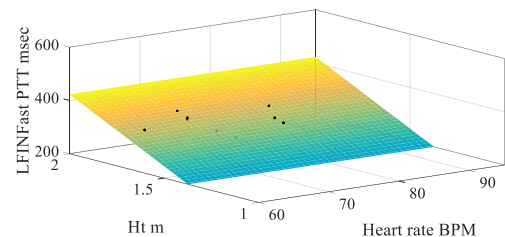


Figure 7.8 Left Finger PTT of 7 fasting subjects  $R = 0.6$ .

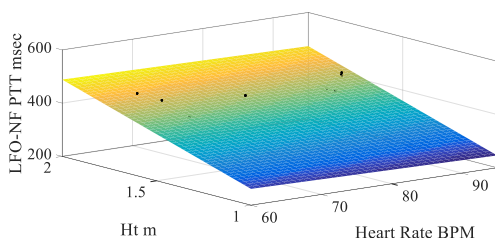


Figure 7.3 Left Foot PTT of 7 non-fasting subjects  $R = 0.6$ .

Figure 7.0 PTT for 7 subjects when not fasting 7.1-7.4 and when fasting 7.5-7.8, as a function of BPM and Ht.

In another small experiment involving two subjects differing in age (see Table 8.0), PTTs and blood pressures were measured from 10 am to 5:30 pm, one measurement every hour. The blood pressure drops with fasting while PTT increases with fasting for the 25 years old,  $p < 0.05$ . Fasting causes hydration a drop in body fluid. The opposite occurs for the 60 years old as arterial stiffness increases with age and possible with fasting. In future large scale PTT fasting studies, subjects may be grouped according to age.

In a recent study on arterial stiffness and hydration [24], it was shown that hydration affected central pressure wave velocity (or PTT) in normothermic resting conditions.

Table 8.0 Whole day PTT and SBp measurements (mean  $\pm$  sd) in fasting and non-fasting days.

Subject No.	Age Years	Height meters	SBp-NF mmHg	LFO-NF PTT msec	SBpFast mmHg	LFOFast PTT msec
1	25	1.65	124 $\pm$ 3	369 $\pm$ 29	119 $\pm$ 4	418 $\pm$ 42
2	60	1.74	124 $\pm$ 4	430 $\pm$ 61	132 $\pm$ 6	401 $\pm$ 21

## VI. CONCLUSION

We designed a dedicated ECG-PPG system that showed acceptable pulse transient time measurements, in a preliminary fasting study. Although the number of subjects participated in the trial is small, Ramadan fasting PTT measurements were shorter in comparison to those measurements after Ramadan. This result is augmenting the fact that the systolic blood pressure is higher in Ramadan compared to that after Ramadan. In what would be a similar major study, the number of participants has to increase, and SBp-PTT measurement must be continuous hour by hour over the month of Ramadan. In this case, the PTT device must be wearable and water-proof, as Muslims wash limbs five times a day.

## ACKNOWLEDGMENT

We would like to thank all the participants from the staff and the students who agreed to be involved in the experiments. Also, we would like to take this opportunity to thank Dr. Mohmmad Bakri from management and business administration college for his advice on the statistical analysis.

## REFERENCES

- Allen J. Photoplethysmography and its application in clinical physiological measurement. *Physiol. Meas.* 2007, 28 R1–R39.
- Mukkamala R., Hahn J. O., Inan O. T., Mestha L. K., Kim C. S., Töreyn H., Kyal S. Towards Ubiquitous Blood Pressure Monitoring via Pulse Transit Time: Theory and Practice. *IEEE Trans Biomed Eng.* August 2015; 62(8): 1879-1901. doi:10.1109/TBME.2015.2441951.
- Sharma M., Barbosa K., Ho V., Griggs D., Ghirmai T., Krishnan S., Hsiai T., Chiao J., and Cao H. Cuff-Less and Continuous Blood Pressure Monitoring: A Methodological Review. *Technologies* 2017, 5, 21.
- Zhang Q., Zhou D., and Zeng X. Highly wearable cuff-less blood pressure and heart rate monitoring with single-arm electrocardiogram and photoplethysmogram signals. *BioMed Eng OnLine* 2017, 16:23 DOI 10.1186/s12938-017-0317-z.
- Hennig, A. and Patzak, A. Continuous blood pressure measurement using pulse transit time. *Somnologie* 2013, 17: 104-110.
- Tang Z., Tamura T., Sekine M., Huang M., Chen W., Yoshida M., Sakatani K., Kobayashi H., and Kanaya S. Chair-based Unobtrusive Cuffless Blood Pressure Monitoring System Based on Pulse Arrival Time. *IEEE Journal of Biomedical and Health Informatics* October 2016, DOI: 10.1109/JBHI.2016.2614962.
- Kao Y. H., Chao P. C. P., and Wey C. L. Design and Validation of a New PPG Module to Acquire High-Quality Physiological Signals for High-Accuracy Biomedical Sensing. *Topics In Quantum Electronics*, January/February 2019. Vol. 25, No. 1, DOI:10.1109/JSTQE.2018.2871604
- Geddes, L. A. *Handbook of Blood Pressure Measurement*; Springer Science & Business Media: Berlin, Germany, 1991.
- Moens, A. I. *Die Pulskurve*; EJ Brill: Leiden, The Netherlands, 1878.
- Nichols, W. W.; O'Rourke, M. F.; Kenney, W. L. *McDonald's Blood Flow in Arteries: Theoretical, Experimental and Clinical Principles*, 3rd ed. J. Cardiopulm. Rehabil. Prev. 1991, 11, 407.

- Keener J. and Sneyd J., *Mathematical Physiology*. New York, USA: Springer-Verlag, 1998.
- WIBMER T., DOERING K., KROPF-SANCHEN C., RÜDIGER S., BLANTA I., STOIBER K. M., ROTTBAUER W., and SCHUMANN C. Pulse Transit Time and Blood Pressure During Cardiopulmonary Exercise Tests. *Physiol. Res.* 2014, 63: 287-296.
- Langewouters, G. J.; Wesseling, K.H', Goedhard, W'JA' The static elastic properties of 45 human thoracic and 20 abdominal aortas in vitro and the parameters of a new model. *J. Biomech.* 1984, 17:425-435.
- Zunyi Tang, Toshiyo Tamura, Masaki Sekine, Ming Huang, Wenxi Chen, Masaki Yoshida, Kaoru Sakatani, Hiroshi Kobayashi, and Shigehiko Kanaya. A Chair-based Unobtrusive Cuffless Blood Pressure Monitoring System Based on Pulse Arrival Time. *IEEE Journal of Biomedical and Health Informatics* October 2016 DOI:10.1109/JBHI.2016.2614962
- Asmar R., Benetos A., J. Topouchian J., Laurent P., Pannier B., Brisac A.M., Target R., and Levy B.I., "Assessment of arterial distensibility by automatic pulse wave velocity measurement validation and clinical application studies," *Hypertension*, 1995, vol. 2, no. 3, pp. 485–490.
- Williams TD, Chambers J. B., May O. I., et al: Concurrent reduction in blood pressure and metabolic rate during fasting in the unrestrained SHR. *Am J Physiol Regulatory Integrative Comp Physiol* 2000, 275: R255-R265.
- Fatima Samad, Fahd Qazi, Mohammad B. Pervaiz, Danesh K. Kella, Maryah Mansoor, Bushra Z. Osmani, Fazia Mir, Muhammad Masood Kadi. EFFECTS OF RAMADAN FASTING ON BLOOD PRESSURE IN NORMOTENSIVE MALES *J. Ayub Med Coll Abbottabad* 2015, 27(2).
- Husain R, Cheah S. H., Duncan T.: Cardiovascular reactivity in Malay Moslems during Ramadan. *Singapore Med J* 1996, 37(4): 398-401,
- Seker, Ayse, Demirci, Hakan, Ocakoglu, Gokhan, Aydin, Ufuk, Ucar, Hakan, Yildiz, Gursel, Yaman, Ozen. Effect of fasting on 24-h blood pressure values of individuals with no previous history of hypertension *Blood Pressure Monitoring. Clinical Methods and Pathophysiology.* October 2017 - Volume 22 - Issue 5 - p 247–252 doi: 10.1097/MBP.0000000000000244
- John Allen et al. Photoplethysmography detection of lower limb peripheral arterial occlusive disease: a comparison of pulse timing, amplitude and shape characteristics. *Physiol. Meas.* 2005, 26 8-11.
- Eilers P. A perfect Smoother. *Anal. Chem.* 2003, 75(14), pp 3631-3636.
- Sedghamiz, H. "Matlab Implementation of Pan Tompkins ECG QRS detector.", March 2014. [https://www.researchgate.net/publication/313673153\\_Matlab\\_Implementation\\_of\\_Pan\\_Tompkins\\_ECG\\_QRS\\_detect](https://www.researchgate.net/publication/313673153_Matlab_Implementation_of_Pan_Tompkins_ECG_QRS_detect)
- Allen, J., & Murray, A. Age-related changes in peripheral pulse timing characteristics at the ears, fingers and toes. *Journal of Human Hypertension* (2002) 16,711-717.
- Caldwell A. R. et al. Hydration status influences the measurement of arterial stiffness. *Clin Physiol Funct Imaging* (2018) 38, pp447-454.